

Linkage Isomerization Reactions of (Acetone)pentaammineruthenium(III) and -ruthenium(II) Complexes

David W. Powell and Peter A. Lay*

Department of Inorganic Chemistry, University of Sydney, Sydney, NSW 2006, Australia

Received April 14, 1992

A complete kinetic and thermodynamic analysis of the linkage isomerizations of $[\text{Ru}(\text{NH}_3)_5(\text{acetone})]^{3+/2+}$ is presented. Each oxidation state exists as two linkage isomers in which acetone is bound via O in an η^1 fashion (favored by Ru(III)) and via C and O of the carbonyl group in an η^2 fashion (favored by Ru(II)). The $[\text{Ru}(\text{NH}_3)_5(\eta^2\text{-OC}(\text{CH}_3)_2)]^{2+}$ and $[\text{Ru}(\text{NH}_3)_5(\eta^1\text{-OC}(\text{CH}_3)_2)]^{3+}$ complexes were characterized by spectroscopic methods (IR, UV/vis, and NMR), and the kinetic and thermodynamic data for these isomerizations were obtained by electrochemical methods. In acetone, the $[\text{Ru}(\text{NH}_3)_5(\eta^2\text{-OC}(\text{CH}_3)_2)]^{3+/2+}$ couple is observed at $E_{1/2} = -337$ mV as ferrocenium/ferrocene (Fc⁺/Fc) at 25 °C, while the $[\text{Ru}(\text{NH}_3)_5(\eta^1\text{-OC}(\text{CH}_3)_2)]^{3+/2+}$ couple is observed at $E_{1/2} = -478$ mV (vs Fc⁺/Fc at 25 °C). For the $\eta^1 \rightarrow \eta^2$ linkage isomerization of $[\text{Ru}(\text{NH}_3)_5(\text{acetone})]^{2+}$, the rate and equilibrium constants at 25 °C in acetone and the enthalpy and entropy of activation are 18 ± 1 s⁻¹, 16 ± 1 , 63 ± 1 kJ mol⁻¹, and -10 ± 2 J K⁻¹ mol⁻¹, respectively. Similarly, for the $\eta^2 \rightarrow \eta^1$ linkage isomerization of $[\text{Ru}(\text{NH}_3)_5(\text{acetone})]^{3+}$, they are 0.46 ± 0.03 s⁻¹, 14 ± 1 , 48 ± 2 kJ mol⁻¹, and -91 ± 7 J K⁻¹ mol⁻¹, respectively. The rate constant for the exchange of coordinated acetone with free acetone in the Ru(III) complex is $(6.9 \pm 0.5) \times 10^{-6}$ s⁻¹, at 0 °C. This is much slower than the Ru(III) $\eta^1 \rightarrow \eta^2$ isomerization rate, $(4.3 \pm 0.4) \times 10^{-3}$ s⁻¹, at the same temperature, indicating an intramolecular isomerization. In a 50% v/v acetone/acetonitrile mixture, at 3 °C, the Ru(II) $\eta^1 \rightarrow \eta^2$ isomerization rate is 0.3 s⁻¹, while the rate constant for the substitution of the coordinated acetone is 0.4 s⁻¹. Therefore, it was not possible to distinguish between an intra- and an intermolecular process. IR spectroscopy and other evidence indicate that the η^2 complex is stabilized by both π -back-bonding and σ -bonding via the ketone double bond, with the latter being more important. At -23 °C, a second ECE process is observed involving the $[\text{Ru}(\text{NH}_3)_5(\text{OSO}_2\text{CF}_3)]^{2+/+}$ couple ($E_{1/2} = -494$ mV vs Fc⁺/Fc) and the η^2 -acetone complex; the rate constant for the substitution of the triflate ligand, in the Ru(II) complex, by acetone was found to be 1.2 ± 0.2 s⁻¹, compared to 0.109 s⁻¹ for the Ru(II) linkage isomerization under the same conditions. The analogous hexafluoroacetone complexes exist entirely in the η^2 form and have redox characteristics similar to those of the η^2 -acetone complexes.

Introduction

The $[\text{Ru}(\text{NH}_3)_5(\text{acetone})]^{3+/2+}$ complexes are useful synthetic intermediates for the preparation of a variety of pentaammineruthenium and decaamminediruthenium complexes.^{1,2} However, it has been observed qualitatively that $[\text{Ru}(\text{NH}_3)_5(\text{acetone})]^{2+}$, in acetone solutions, undergoes substitution reactions at rates that are comparable to those observed for $[\text{Ru}(\text{NH}_3)_5(\text{OH}_2)]^{2+}$ in water.³ This is a surprising result, since the acetone ligand is normally a much better leaving group than the aqua ligand.⁴ At the same time, it was noticed that the reduction of $[\text{Ru}(\text{NH}_3)_5(\text{acetone})]^{3+}$ appeared to follow an ECEC mechanism.³ As a consequence of these anomalous behaviors, the known affinity of the pentaammineruthenium(II) moiety for π -back-bonding,⁵ and the recent isolation of the η^2 -acetone complex $[\text{Os}(\text{NH}_3)_5(\eta^2\text{-OC}(\text{CH}_3)_2)]^{2+}$,^{6,7} the nature of Ru(III)/Ru(II) acetone complexes has been investigated in detail by both electrochemical and spectroscopic techniques. A preliminary account of this chemistry has been reported elsewhere.⁸ Here we report details of the substitution chemistry and linkage isomerization reactions

of $[\text{Ru}(\text{NH}_3)_5(\text{acetone})]^{3+/2+}$ complexes. These indicate that the contributions of σ -bonding via the double bond and π -back-bonding to the stabilization of the η^2 -C,O acetone complexes in the Ru and Os systems are quite different. This is also the first complete characterization of the thermodynamics and kinetics of such isomerization reactions involving aldehyde or ketone ligands.

Experimental

Reagents. $[\text{Ru}(\text{NH}_3)_5(\text{OSO}_2\text{CF}_3)](\text{CF}_3\text{SO}_3)_2$ was synthesized from $[\text{Ru}(\text{NH}_3)_6]\text{Cl}_3$ (Aldrich, 98%) as described in the literature.^{2,9} Acetone (Aldrich, HPLC grade), acetonitrile (Aldrich, HPLC grade), and hexafluoroacetone trihydrate (Aldrich, 98%) were used as supplied, diethyl ether (Ajax Chemicals, AR grade) was dried over Na⁺,¹⁰ and 4-hydroxy-4-methylpentan-2-one (diacetone alcohol or daa; BDH Chemicals, 98%) was dried over K₂CO₃ (Merck, GR grade) and then distilled under reduced pressure.¹¹ Acetone (Aldrich, AR) that was distilled from KMnO₄/CaSO₄ or that had been dried with activated alumina or silica gel powder gave essentially the same results as those obtained with the HPLC grade solvent. However, when AR or HPLC grade acetone was dried over 4-Å molecular sieves, K₂CO₃ or B₂O₃, these promoted the formation of diacetone alcohol and mesityl oxide (for B₂O₃), which competed with acetone

- Callahan, R. W.; Brown, G. M.; Meyer, T. J. *Inorg. Chem.* **1975**, *14*, 1443-1453.
- Lawrance, G. A.; Lay, P. A.; Sargeson, A. M.; Taube, H. *Inorg. Synth.* **1986**, *24*, 257-263.
- Lay, P. A. Unpublished results, 1982.
- Dixon, N. E.; Jackson, W. G.; Lancaster, M. J.; Lawrance, G. A.; Sargeson, A. M. *Inorg. Chem.* **1981**, *20*, 470-476.
- Taube, H. *Pure Appl. Chem.* **1979**, *51*, 901-912; *Comments Inorg. Chem.* **1981**, *1*, 127-131.
- Harman, W. D.; Fairlie, D. P.; Taube, H. *J. Am. Chem. Soc.* **1986**, *108*, 8223-8227.
- Harman, W. D.; Sekine, H.; Taube, H. *J. Am. Chem. Soc.* **1988**, *110*, 2439-2445.

- Powell, D. W.; Lay, P. A. In *Proceedings of the Seventh Australian Electrochemistry Conference (Current and Potential Applications)*; Tran, T.; Skyllas-Kazacos, M., Eds.; Royal Australian Chemical Institute: Sydney, 1981; pp 237-240. Powell, D. W. Ph.D. Thesis, University of Sydney, 1990.
- Dixon, N. E.; Lawrance, G. A.; Lay, P. A.; Sargeson, A. M. *Inorg. Chem.* **1984**, *23*, 2940-2947.
- Gordon, A. J.; Ford, R. A. *The Chemists Companion*; Wiley: New York, 1972.
- Riddick, J. A.; Bunger, W. B. *Organic Solvents*; Wiley-Interscience: New York, 1970.

for coordination. Tetra-1-butylammonium tetrafluoroborate (TBATFB) (Aldrich) was repeatedly recrystallized from ethyl acetate/Et₂O until there was no observable residual current from impurities in the electrochemistry.¹² Tetra-1-butylammonium hexafluorophosphate (TBAHF-P) was prepared from the reaction of Bu₄NOH (40% solution in water, Aldrich) and KPF₆ (EGA Chemicals, 98%) and recrystallized as for TBATFB.¹² Zn(CF₃SO₃)₂·nH₂O was prepared from the reaction of ZnCO₃ and CF₃SO₃H (Aldrich) and then dehydrated over P₄O₁₀.¹³ Acetone-2-¹³C (Aldrich, 99 atom % ¹³C) was used as supplied. Acetone-¹⁸O was synthesized as described in the literature from ¹⁸OH₂ (MSD Isotopes, 97 atom % ¹⁸O).^{6,7} All solvents were thoroughly deoxygenated prior to use by purging with argon. Reactions were performed under an argon atmosphere using Schlenk apparatus and argon/vacuum-line techniques. The argon used was high-purity grade (CIG) and was further purified to remove traces of water and oxygen by passing through a column of sodium dispersed on glass wool.¹⁴

Instrumentation. Infrared spectra (CsI plates/Nujol mulls, polyethylene disks, or KBr disks) were obtained from a Digilab FTS80 FTIR spectrometer. ¹H NMR spectra were recorded on either a 400-MHz Bruker WM400 or a 400-MHz Bruker AMX NMR spectrometer (relative to tetramethylsilane, in ppm). The electronic absorption spectra were recorded on a Cary 17D spectrophotometer. Molar conductivity measurements (in acetone) were obtained using a Philips PW 9506 conductivity meter and calibrated against (1-Bu)₄NBr.¹⁵

Bulk electrolysis and coulometry experiments were performed using a PAR Model 173 potentiostat/galvanostat in conjunction with a PAR Model 179 digital coulometer. A platinum-mesh counter electrode, a platinum-basket working electrode, and a saturated calomel reference electrode were used in these experiments. All other electrochemical experiments were performed on a BAS 100 electrochemical analyzer interfaced with a Houston Instruments DMP-40 digital plotter. A three-electrode system was used with a platinum (1.6-mm diameter) or glassy-carbon (3.2-mm diameter) disk working electrode, a platinum-wire counter electrode, and an Ag/AgCl/KCl(satd) reference electrode. Under the reaction conditions used in acetone, ~80–100% internal resistance (*i*R) compensation was attained with cyclic voltammetry. All reduction potentials were referenced to the Fc⁺/Fc redox couple using the same cell configuration.¹⁶

Variable-temperature electrochemistry was performed in a nonisothermal cell;¹⁷ the reference compartment was maintained at a constant temperature of 25.0 ± 0.1 °C with a B. Braun Thermomix 1419 water bath and the working compartment thermostated (± 0.1 °C) with a Haake D8 Immersion Circulator/Haake EK51 cooler. Four independent runs were performed for each redox couple. The temperature range used for the η² isomer was 3–25 °C, while for the η¹ isomer the range used was –23 to +25 °C.

Synthesis. [Ru(ND₃)₅(OSO₂CF₃)](CF₃SO₃)₂. [Ru(NH₃)₅Cl]Cl₂ (687 mg) was refluxed in D₂O (15 mL) for 30 min; after the mixture was cooled to 25 °C, 5 M HCl (30 mL) was added and the resulting precipitate was filtered off and washed with cold D₂O (5 mL), 5 M HCl (2 × 10 mL), and acetone (20 mL). The solid was then used to prepare [Ru(ND₃)₅(OSO₂CF₃)](CF₃SO₃)₂ using the method described in the literature for the nondeuterated complex.²⁹ A white product was obtained with a yield of 574 mg (94%).

[Ru(NH₃)₅(acetone)](CF₃SO₃)₃. [Ru(NH₃)₅(OSO₂CF₃)](CF₃SO₃)₂ (247 mg) was dissolved in acetone (5 mL), and the solution was allowed to stand for 15 min under argon. Diethyl ether (30 mL) was then added to precipitate a white product. This was filtered off, washed with Et₂O, and dried under vacuum. Yield: 226 mg (84%).

[Ru(NH₃)₅(acetone-2-¹³C)](CF₃SO₃)₃. This was prepared from [Ru(NH₃)₅(OSO₂CF₃)](CF₃SO₃)₂ (90 mg) as for [Ru(NH₃)₅(acetone)](CF₃SO₃)₃ using acetone-2-¹³C (1 mL). Yield: 90 mg (90%).

[Ru(NH₃)₅(acetone)](CF₃SO₃)₂. [Ru(NH₃)₅(OSO₂CF₃)](CF₃SO₃)₂ (411 mg) was dissolved in acetone (5 mL) under argon, and the solution of [Ru(NH₃)₅(acetone)]³⁺ formed was then reduced with Zn(Hg) for 1

h. A pale yellow solid was obtained upon the addition of deaerated Et₂O (30 mL). This was filtered off, washed with Et₂O, and dried under vacuum and stored over Ar. Yield: 240 mg (69%).

[Ru(NH₃)₅(acetone-¹⁸O)](PF₆)₂. This was prepared from [Ru(NH₃)₅(OC(CH₃)₂)](PF₆)₂ (95 mg) using a modification of the reported method¹⁸ with 1 mL of acetone-¹⁸O as the solvent. Yield: 50 mg (52%).

[Ru(ND₃)₅(acetone)](PF₆)₂. This was prepared as above using [Ru(ND₃)₅(OSO₂CF₃)](CF₃SO₃)₂ and isolated by the successive addition of KPF₆ and Et₂O. Yield: 90 mg (55%).

The acetone complexes were too reactive to obtain satisfactory microanalytical data, but IR and NMR spectroscopies and electrochemistry all indicated that the complexes were relatively pure (see Results).

[Ru(NH₃)₅(OH₂)](CF₃SO₃)₃. [Ru(NH₃)₅(OSO₂CF₃)](CF₃SO₃)₂ (282 mg) was dissolved in a 0.1 M aqueous solution of CF₃SO₃H (1 mL). After the solution was cooled to <5 °C, neat CF₃SO₃H (1 mL) was slowly added, with stirring. The mixture was kept at <5 °C overnight, and the resulting white product was filtered off, air-dried, washed with diethyl ether, and stored over P₄O₁₀. Yield: 168 mg (58%).

[Ru(NH₃)₅(OC(CF₃)₂)](PF₆)₂. [Ru(NH₃)₅(OH₂)](PF₆)₃ (271 mg) was dissolved in a mixture of acetone (12 mL) and hexafluoroacetone trihydrate (3 mL) under argon. The solution of [Ru(NH₃)₅(solvent)]³⁺ was reduced with Zn(Hg) for 30 min, whereupon diethyl ether (50 mL) was added to precipitate out the pale yellow product, which was then isolated as for the analogous complex. Yield: 207 mg (76%).

[Ru(NH₃)₅(acetone)]³⁺ and [Ru(NH₃)₅(acetone)]²⁺. For electrochemical and solution spectroscopy measurements, these were prepared in situ under argon. [Ru(NH₃)₅(acetone)]³⁺ was formed by the solvolysis of [Ru(NH₃)₅(OSO₂CF₃)](CF₃SO₃)₂ in acetone.² [Ru(NH₃)₅(acetone)]²⁺ was formed by the Zn(Hg) reduction of [Ru(NH₃)₅(acetone)]³⁺.²

[Ru(NH₃)₅(OC(CF₃)₂)]³⁺ and [Ru(NH₃)₅(OC(CF₃)₂)]²⁺. These were prepared in a 50% v/v acetone/hexafluoroacetone trihydrate mixture in the same manner as for the acetone complexes.

[Ru(NH₃)₅(daa)]³⁺ and [Ru(NH₃)₅(daa)]²⁺. These were prepared in diacetone alcohol in a manner similar to that for the acetone complexes.

Kinetic and Thermodynamic Experiments. The two methods of Nicholson and Shain¹⁹ for EC systems were used to calculate the rate constants for the isomerization reactions and the substitution reactions of the Ru(III) complexes. In the first method, the rate constants were derived from the ratio of forward to reverse peak currents in cyclic voltammograms when the voltammograms were in the near-reversible regimes. Peak currents were estimated by approximating the charging current as a curve. The second method involved determining the rate constants from the shift of the forward peak potential relative to E_{1/2}.¹⁹

Equilibrium constants were also determined using two different techniques. In the first, they were obtained from the first derivatives of normal-pulse voltammograms, where the sampling was faster than the isomerization process, hence yielding the equilibrium concentrations of the two isomers in each oxidation state.²⁰ The second method used was based upon that of Laviron.²¹ At slow scan rates a single pseudoreversible system was observed at a potential of E_K, which is a function of the two equilibrium constants. The two equilibrium constants were then calculated using the equations

$$E_K = E_1 - (RT/F) \ln(1 + K_1) \quad (1)$$

$$E_K = E_2 + (RT/F) \ln(1 + K_2) \quad (2)$$

Rate constants (*k*₁, *k*₂) at 21 and 25 °C were averaged from at least 10 measurements, all other kinetic and thermodynamic data were averaged from at least four measurements using a thermostated nonisothermal cell. Standard deviations in all cases were less than 5%.

(18) Baumann, J. A.; Meyer, T. J. *Inorg. Chem.* **1980**, *19*, 345–350.

(19) Nicholson, R. S.; Shain, I. *Anal. Chem.* **1964**, *36*, 706–723. The method, as described by Nicholson and Shain, applies to cyclic voltammetry; however, the BAS-100 instrument utilizes cyclic staircase voltammetry. Under the conditions used, the step size is sufficiently small that any error arising from this difference is within the experimental error, as shown by the similarity of the values obtained using the two different methods (Christie, J. H.; Lingane, P. J. *J. Electroanal. Chem. Interfacial Electrochem.* **1965**, *10*, 176–182).

(20) Magnuson, R. H.; Mierowitz, R.; Zulu, S.; Giering, W. P. *J. Am. Chem. Soc.* **1982**, *104*, 5790–5791.

(21) Vallat, A.; Person, M.; Roullier, L.; Laviron, E. *Inorg. Chem.* **1987**, *26*, 332–335.

(12) Moulton, R.; Wiedman, T. W.; Vollhardt, P. C.; Bard, A. J. *Inorg. Chem.* **1986**, *25*, 1846–1849.

(13) Lay, P. A. Ph.D. Thesis, Australian National University, 1981. Jackson, W. G.; Lawrence, G. A.; Lay, P. A.; Sargeson, A. M. *Aust. J. Chem.* **1982**, *35*, 1561–1580.

(14) Storch, H. H. *J. Am. Chem. Soc.* **1934**, *56*, 374–378.

(15) Reynolds, M. B.; Kraus, C. A. *J. Am. Chem. Soc.* **1948**, *70*, 1709–1713.

(16) IUPAC Commission on Electrochemistry (U.K.). *Pure Appl. Chem.* **1984**, *56*, 461–466.

(17) Yee, E. L.; Cave, R. J.; Guyer, K. L.; Tyma, P. D.; Weaver, M. J. *J. Am. Chem. Soc.* **1979**, *101*, 1131–1137.

Table I. Infrared Spectral Data (cm⁻¹)

complex		R = D	R = H
[Ru(NH ₃) ₅ (OC(CH ₃) ₂)](CF ₃ SO ₃) ₃ ^a	ν_{NR}	2469, 2366	3304
	ν_{CO}	1703	1692 (1630) ^b
	$\delta_{(\text{RNR})_{\text{as}}}$	1198	1627
	$\delta_{(\text{RNR})_{\text{s}}}$	c	1363
	ρ_{NR}	649	813
	ν_{NR}	2360 ^a	3250 ^d
	$\delta_{(\text{RNR})_{\text{as}}}$	1193	1627
[Ru(NH ₃) ₅ (OC(CH ₃) ₂)](PF ₆) ₂	ν_{CO}	1285	1677 (η^1) 1277 (η^2) (1230) ^e
	$\delta_{(\text{RNR})_{\text{s}}}$	991	1265 sh
	ρ_{NR}	638	780 sh
	$\nu_{\text{Ru-N}}$		505, 478, 472
	$\nu_{\text{Ru-O}}$		396
	δ_{NRuN}		255
	ν_{NR}		3340, 3280
	$\delta_{(\text{RNR})_{\text{as}}}$		1645
	ν_{CO}		1363
	$\delta_{(\text{RNR})_{\text{s}}}$		1222
[Ru(NH ₃) ₅ (OC(CF ₃) ₂)](PF ₆) ₂ ^d	ρ_{NR}		780 sh
	$\nu_{\text{Ru-N}}$		509, 475
	$\nu_{\text{Ru-O}}$		399
	δ_{NRuN}		255
	ν_{NR}		1645
	$\delta_{(\text{RNR})_{\text{as}}}$		1363
	ν_{CO}		1222

^a Recorded as Nujol mulls, with CsI plates. ^b 2-¹³C-labeled acetone complex. ^c Obscured by CF₃SO₃⁻. ^d Recorded as KBr disk. ^e ¹⁸O-labeled acetone complex. \parallel = O=C.

The rate constants for the substitution of triflate by acetone and the substitution of acetone in [Ru(NH₃)₅(η^1 -acetone)]²⁺ by acetonitrile, in a 50% v/v acetone/acetonitrile solution, were obtained from cyclic voltammetry, using the method of Nicholson and Shain.¹⁹

The substitution of acetone in [Ru(NH₃)₅(η^1 -acetone)]²⁺ by acetone-*d*₆ at 0 and 5 °C, was followed by the loss of the methyl signal of the coordinated acetone in the ¹H NMR spectrum, calibrated using a trace of ethanol.

Results

Spectroscopy. The infrared spectrum of [Ru(NH₃)₅(OC(CH₃)₂)](CF₃SO₃)₃ (Table I) exhibits a peak at 1690 cm⁻¹, which is characteristic of the carbonyl stretch of η^1 -coordinated acetone.²² Upon ¹³C labeling of the carbonyl group, this stretch shifts to ~1631 cm⁻¹. The infrared spectrum of [Ru(NH₃)₅(OC(CH₃)₂)](PF₆)₂ (Table I) contains a very weak peak at 1677 cm⁻¹, which is consistent with η^1 -coordinated acetone,²² and an additional medium-intensity peak that is observed at 1277 cm⁻¹. The latter shifts to 1230 cm⁻¹ upon ¹⁸O labeling of the acetone ligand and is characteristic of η^2 -coordinated acetone.⁶ This assignment is supported by the observation of a similar value for the C=O stretch of sideways-bound acetone on a Ru(001) surface (1290 cm⁻¹).²³ The peak due to the C=O stretch of free acetone (1725 cm⁻¹)²⁴ was either absent or extremely weak, indicating that there was little, if any, free acetone present in the complexes. The infrared spectrum of the hexafluoroacetone complex, [Ru(NH₃)₅(OC(CF₃)₂)](PF₆)₂, exhibits an intense peak at 1363 cm⁻¹ and peaks also at 509, 475, 399, and 255 cm⁻¹, in the far-infrared region. The far-infrared region of [Ru(NH₃)₅(OC(CH₃)₂)](PF₆)₂ contains peaks at 505, 478, 472, 396, and 255 cm⁻¹, with intensities similar to those of the peaks of the hexafluoroacetone complex.

The UV-visible spectrum of [Ru(NH₃)₅(OC(CH₃)₂)](CF₃SO₃)₃, in acetone, exhibits a peak at 361.5 nm ($\epsilon_{\text{max}} = 3.9 \times 10^3 \text{ M}^{-1} \text{ cm}^{-1}$) and a shoulder at 413 nm ($\epsilon_{\text{max}} \sim 4.7 \times 10^2 \text{ M}^{-1} \text{ cm}^{-1}$); the latter is characteristic of a [Ru(NH₃)₅L]²⁺ d-d transition.²⁵ The intensity and wavelength of the peak at 361.5

nm are within the range expected for a charge-transfer transition,²⁵ in this case the d → π^* transition. With time, two peaks at 386 and 503 nm appeared; the appearance and position of these peaks are consistent with the formation of [(NH₃)₅RuORu(NH₃)₅]⁴⁺ complexes due to the rapid reaction with traces of O₂.¹⁸ The UV-visible spectrum of [Ru(NH₃)₅(OC(CH₃)₂)](CF₃SO₃)₃, in acetone, exhibits a single peak at 327 nm ($\epsilon_{\text{max}} = 3.2 \times 10^2 \text{ M}^{-1} \text{ cm}^{-1}$).

The ¹H NMR spectrum of paramagnetic [Ru(NH₃)₅(OC(CH₃)₂)](CF₃SO₃)₃ was examined in a number of solvents. A peak assignable to the cis NH₃ was observed at 121 ppm. The trans NH₃ resonance was not observed; however, the absence of this peak has been noted before in other pentaammineruthenium(III) complexes.^{26,27} Only one signal was observed for the methyls of the acetone ligand, indicating a rapid rotation around the Ru-O bond.⁶ The ¹H NMR spectra of [Ru(NH₃)₅(OC(CH₃)₂)](CF₃SO₃)₃ dissolved in both acetone-*d*₆ (at 0 °C, to prevent ligand exchange) and undeuterated acetone (at 25 °C) exhibit two peaks in the ratio of [~5 (121.2 ppm)]:[2 (3.47 ppm)] which are assignable to the ammine and the methyl groups, respectively. At 25 °C, the coordinated acetone is displaced by the solvent within the time taken to run the experiment and the peaks due to free acetone in D₂O, acetone-*d*₆, and *N,N*-dimethylformamide-*d*₇ exist in the ratio ~2:5 relative to the ammine signal, indicating quantitative displacement of the acetone ligand at 25 °C. Attempts to obtain the ¹³C NMR spectrum of the 2-¹³C-labeled Ru(III) acetone complex, in acetone-*d*₆ at 0 °C, were unsuccessful, with the C=O resonance being shifted beyond the available range (+1200 → -600 ppm) or broadened too much to be observed. The growth, with time, of the solvent C=O resonance due to the release of the (CH₃)₂¹³CO ligand confirmed, indirectly, the presence of the coordinated ligand.

The ¹H NMR spectrum of [Ru(NH₃)₅(OC(CH₃)₂)]²⁺ in undeuterated acetone at 0 °C exhibits two resonances at 3.18 and 2.81 ppm in the ratio 1:4, consistent with cis and trans amines, but not a discernible methyl resonance due to uncoordinated acetone.²⁵ At -60 °C, the ammine peaks were shifted to 3.76 (trans) and 2.99/3.05 ppm (cis, split), and an additional peak also appeared at 1.78 ppm, which has been assigned to the coordinated acetone. The methyl resonance and the split cis ammine signals first appeared at -20 °C. In other experiments, the presence of acetone has also been confirmed by the observation of a peak at ~2.1 ppm at 25 °C due to acetone displaced from [Ru(NH₃)₅(acetone)]²⁺ dissolved in D₂O/DCl, acetone-*d*₆, and *N,N*-dimethylformamide-*d*₇.

Conductivity. The molar conductivity of [Ru(NH₃)₅(OC(CH₃)₂)](CF₃SO₃)₃, in acetone, was found to be $94 \pm 1 \text{ S cm}^2 \text{ mol}^{-1}$, which is similar to that of [Ru(NH₃)₆](CF₃SO₃)₃ ($99 \pm 1 \text{ S cm}^2 \text{ mol}^{-1}$ in acetone), indicating the presence of a neutral ligand.

Electrochemistry. Coulometry experiments on the reduction of [Ru(NH₃)₅(OC(CH₃)₂)](CF₃SO₃)₃, in acetone at -140 mV (relative to SCE), resulted in a one-electron reduction ($n = 0.97 \pm 0.02$).

The sensitivity of both oxidation states to reactions with impurities in the acetone required careful attention to solvent purity. Common impurities such as water and alcohols were found to readily displace the acetone ligand in both complexes. These were overcome by the use of HPLC grade acetone (Aldrich).

At slow scan rates (<2 V s⁻¹) and at 25 °C, the cyclic voltammetry of [Ru(NH₃)₅(OC(CH₃)₂)]³⁺ exhibits reduction and oxidation processes with $\Delta E_p \sim 200 \text{ mV}$ (Figure 1B). A similar response is obtained from the cyclic voltammetry of

(22) Bennett, M. A.; Matheson, T. W.; Robertson, G. B.; Steffan, W. L.; Turney, T. W. *J. Chem. Soc., Chem. Commun.* **1979**, 32-33.

(23) Avery, N. R.; Wienberg, W. H.; Anton, A. B.; Toby, B. H. *Phys. Rev. Lett.* **1983**, *51*, 682-687.

(24) Dellepiane, G.; Overend, J. *Spectrochim. Acta* **1966**, *22*, 593-614.

(25) Lehmann, H.; Schenk, K. J.; Chapuis, G.; Ludi, A. *J. Am. Chem. Soc.* **1979**, *101*, 6197-6202.

(26) Clarkson, S.; Hush, N. S.; Lay, P. A. Unpublished results, University of Sydney.

(27) Toi, H.; La Mar, G. N.; Margalit, R.; Che, C.-M.; Gray, H. B. *J. Am. Chem. Soc.* **1984**, *106*, 6213-6217.

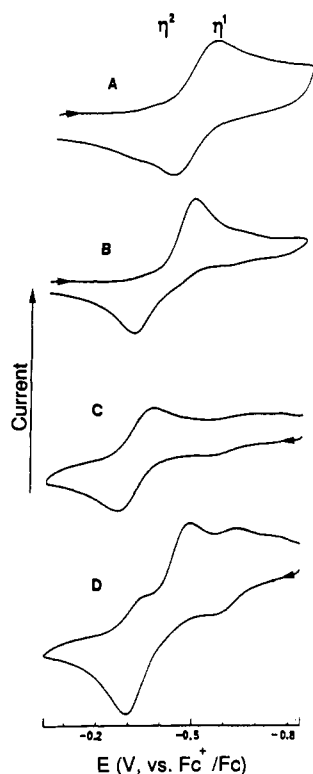


Figure 1. Cyclic voltammograms, in acetone at 25 °C, vs Fc^+/Fc (2 mM electroactive species, 0.1 M (1-Bu) $_4\text{NBF}_4$): A, $[\text{Ru}(\text{NH}_3)_5(\text{OC}(\text{CH}_3)_2)]^{3+}$ at 51.2 V s^{-1} ; B, $[\text{Ru}(\text{NH}_3)_5(\text{OC}(\text{CH}_3)_2)]^{3+}$ at 100 mV s^{-1} ; C, $[\text{Ru}(\text{NH}_3)_5(\text{OC}(\text{CH}_3)_2)]^{2+}$ at 2.53 V s^{-1} ; D, $[\text{Ru}(\text{NH}_3)_5(\text{OC}(\text{CH}_3)_2)]^{2+}$ at 100 mV s^{-1} .

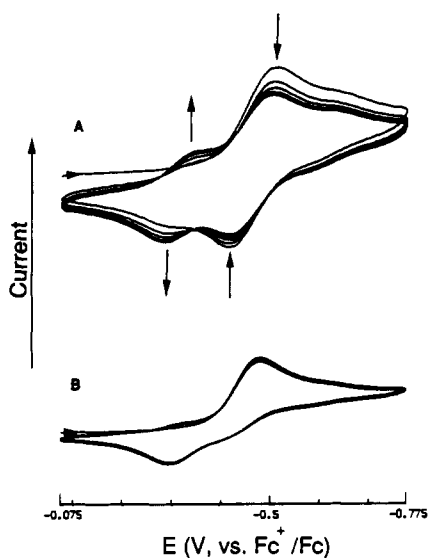
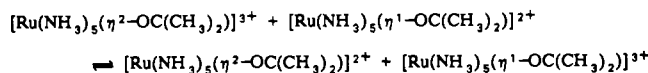
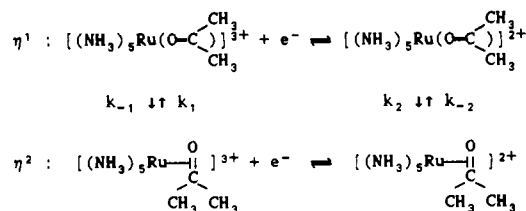


Figure 2. Multiscan cyclic voltammograms, in acetone at 21 °C, vs Fc^+/Fc (2 mM electroactive species, 0.1 M (1-Bu) $_4\text{NBF}_4$, five scans): A, $[\text{Ru}(\text{NH}_3)_5(\text{OC}(\text{CH}_3)_2)]^{3+}$ at 5.12 V s^{-1} ; B, $[\text{Ru}(\text{NH}_3)_5(\text{OC}(\text{CH}_3)_2)]^{2+}$ at 100 mV s^{-1} .

$[\text{Ru}(\text{NH}_3)_5(\text{OC}(\text{CH}_3)_2)]^{2+}$, at slow scan rates ($<500 \text{ mV s}^{-1}$) (Figure 1D). However, at faster scan rates, both complexes display reversible cyclic voltammograms; for $[\text{Ru}(\text{NH}_3)_5(\text{OC}(\text{CH}_3)_2)]^{3+}$ at 51.2 V s^{-1} , a couple is observed at -479 mV (Fc^+/Fc), while, for $[\text{Ru}(\text{NH}_3)_5(\text{OC}(\text{CH}_3)_2)]^{2+}$ at 1003 mV s^{-1} , a couple is observed at -337 mV (Fc^+/Fc , Figure 1A,C). The reversibility of the conversions between the two chemical forms of the system was shown by the use of multiscan cyclic voltammetry (Figure 2). With time, in Ru(III) solutions, a third couple is observed at -614 mV which is consistent with the OH-bound complex of diacetone alcohol, since cyclic voltammetry of $[\text{Ru}(\text{NH}_3)_5(\text{OSO}_2\text{CF}_3)](\text{CF}_3\text{SO}_3)_2$ dissolved in diacetone alcohol

Scheme I. Square Reaction Scheme for the Linkage Isomerization Reactions of Acetone Complexes



gives rise to reversible couples at -613 ± 5 and $-303 \pm 5 \text{ mV}$.²⁸ The cyclic voltammograms of the hexafluoroacetone complexes $[\text{Ru}(\text{NH}_3)_5(\text{OC}(\text{CF}_3)_2)]^{3+}$ and $[\text{Ru}(\text{NH}_3)_5(\text{OC}(\text{CF}_3)_2)]^{2+}$, in 50% acetone/hexafluoroacetone trihydrate, exhibit a single, reversible couple at -283 mV (Fc^+/Fc). The $[\text{Ru}(\text{NH}_3)_5(\text{OH}_2)]^{3+/2+}$ couple is found at -400 mV (Fc^+/Fc) in acetone.

Kinetics and Thermodynamics. The scan-rate-dependent reversibility noted above is characteristic of an ECEC mechanism or square reaction scheme.²⁹ Oxidation-state-dependent linkage isomerizations in which there is a rapid isomerization of the acetone ligand to η^2 -coordination upon reduction and a corresponding isomerization to η^1 -coordination upon oxidation are apparent (see Discussion and Scheme I). Rate constants were determined using the two independent methods of Nicholson and Shain for EC systems.¹⁹ Both methods yielded identical results (Table II): for the $\eta^1 \rightarrow \eta^2$ linkage isomerization of $[\text{Ru}(\text{NH}_3)_5(\text{OC}(\text{CH}_3)_2)]^{2+}$ following the reduction of $[\text{Ru}(\text{NH}_3)_5(\text{OC}(\text{CH}_3)_2)]^{3+}$, the rate constant, k_2 , was found to be $16 \pm 1 \text{ s}^{-1}$, while, for the $\eta^2 \rightarrow \eta^1$ linkage isomerization of $[\text{Ru}(\text{NH}_3)_5(\text{OC}(\text{CH}_3)_2)]^{3+}$, following the oxidation of $[\text{Ru}(\text{NH}_3)_5(\text{OC}(\text{CH}_3)_2)]^{2+}$, the rate constant, k_1 , was determined to be $0.46 \pm 0.03 \text{ s}^{-1}$ (both at 25 °C). Equilibrium constants for the two isomerizations were also calculated by two independent methods. In the first, they were obtained from the first derivatives of normal-pulse voltammograms,²⁰ while the second method used was that of Laviron.²¹ In both cases the results were identical (Table III): for the $\eta^1 \rightarrow \eta^2$ isomerization of $[\text{Ru}(\text{NH}_3)_5(\text{OC}(\text{CH}_3)_2)]^{2+}$, the equilibrium constant, K_2 , was found to be 16 ± 1 ($\Delta G^\circ = -6.9 \pm 0.2 \text{ kJ mol}^{-1}$), and for the $\eta^2 \rightarrow \eta^1$ isomerization of $[\text{Ru}(\text{NH}_3)_5(\text{OC}(\text{CH}_3)_2)]^{3+}$, K_1 was calculated to be 14 ± 1 ($\Delta G^\circ = -6.5 \pm 0.2 \text{ kJ mol}^{-1}$) (both at 25 °C). The rate constants were measured at two different concentrations of ruthenium, 2.0 and 0.52 mM, both concentrations yielding similar values (Table II). The equilibrium and kinetic data enabled the rate constants for the isomerizations in the reverse directions to be obtained from the principle of microscopic reversibility. At 25 °C, k_{-1} and k_{-2} were calculated to be $0.034 \pm 0.003 \text{ s}^{-1}$ and $1.10 \pm 0.07 \text{ s}^{-1}$, respectively.

The equilibrium constant, K_3 , for the cross-reaction (Scheme I) was also measured. K_3 was calculated both from the product of the equilibrium constants for the two isomerizations, K_1 and K_2 , and from the difference in the redox potentials of the η^1 and η^2 isomers. Both methods yielded a value of 230 ± 20 (at 25 °C).

The possibility that the observed reactions are oxidation-state-dependent substitution reactions involving triflate and acetone ligands was ruled out by the fact that the rate constants for the isomerizations were independent of both the CF_3SO_3^- and electrolyte concentrations (Table II). This was supported by the infrared spectra, which did not show any sign of coordinated

(28) Powell, D. W. Ph.D. Thesis, University of Sydney, 1990.

(29) Jacq, J. *J. Electroanal. Chem. Interfacial Electrochem.* 1971, 29, 149-180.

Table II. Rate Constants for the Linkage Isomerizations of $[\text{Ru}(\text{NH}_3)_5(\text{OC}(\text{CH}_3)_2)]^{3+/2+}$ in Acetone at 21 °C

[Ru], mM	[electrolyte], M	electrolyte counter ion	[added $\text{Zn}(\text{CF}_3\text{SO}_3)_2$], M	k_1 , ^a s ⁻¹	k_2 , ^a s ⁻¹
0.52	0.100	BF_4^-	0.000	0.34 ± 0.04 (11) ^b	15 (1) ^b
2.0	0.0100	BF_4^-	0.000	0.35 ± 0.03 (11) ^b	12 ± 1 (7) ^b
2.0	0.100	PF_6^-	0.000	0.37 ± 0.03 (3) ^b	12.0 ± 0.5 (4) ^b
2.0	0.100	BF_4^-	0.000	0.35 ± 0.06 (6) ^b	11.8 ± 0.9 (15) ^b
2.0	0.100	BF_4^-	0.000	0.33 ± 0.03 (2) ^c	12 ± 1 (7) ^c
2.0	0.100	BF_4^-	0.010	0.35 ± 0.03 (10) ^b	13 ± 1 (12) ^b
2.0	0.100	BF_4^-	~ 0.05 ^d	0.5 ± 0.1 (10) ^b	

^a Number of measurements in parentheses. ^b Determined by Nicholson and Shain, method 1. ^c Determined by Nicholson and Shain, method 2. ^d Effective triflate concentration ~ 0.1 M (saturated).

Table III. Thermodynamics of the $[\text{Ru}(\text{NH}_3)_5(\text{OC}(\text{CH}_3)_2)]^{3+/2+}$ Linkage Isomerizations at 25 °C

isomerization	K	ΔG° ^a	ΔH° ^a	ΔS° ^b	ΔG^\ddagger ^a	ΔH^\ddagger ^a	ΔS^\ddagger ^b
Ru(III) $\eta^2 \rightarrow \eta^1$	13.5 ± 0.5	-6.5 ± 0.2	-7.7 ± 0.2	-4.0 ± 0.2	75 ± 1	48 ± 2	-91 ± 7
Ru(III) $\eta^1 \rightarrow \eta^2$	0.0741	6.5			83 ± 3	55 ± 2	-90 ± 2
Ru(II) $\eta^1 \rightarrow \eta^2$	16.4 ± 0.6	-6.9 ± 0.3	-9.4 ± 0.6	-8.4 ± 0.6	66 ± 7	63 ± 1	-10 ± 2
Ru(II) $\eta^2 \rightarrow \eta^1$	0.061	6.9			73 ± 3	67 ± 2	-19 ± 2
electron-transfer cross-reaction	230 ± 20	-13.6 ± 0.5	-14 ± 1	-1 ± 2			

^a In kJ mol^{-1} . ^b In $\text{J K}^{-1} \text{mol}^{-1}$.

Table IV. Temperature Dependence of the Rate and Equilibrium Constants for the Linkage Isomerizations of $[\text{Ru}(\text{NH}_3)_5(\text{OC}(\text{CH}_3)_2)]^{3+/2+}$

temp, °C	k_1 , ^b s ⁻¹	k_2 , ^b s ⁻¹	K_1	K_2
-23.2		0.112 (6)		
-21.4		0.150 (7)		
-18.8		0.198 (7)		
-16.2		0.269 (4)		
-11.6		0.457 (10)		
-5.3		0.93 (3)		
2.1	0.09 (2)	2.18 (8)	17 (2) ^c	22 (2) ^c
3.8	0.11 (2)	2.46 (16)		
5.8	0.12 (2)	2.66 (6)		
7.8	0.13 (2)	3.70 (5)		
10.0	0.16 (2)	4.50 (10)	15.8 (3) ^c	19.0 (2) ^c
11.8	0.19 (2)	5.7 (3)		
14.2	0.22 (2)			
16.3		9.3 (2)		
18.7	0.30 (2)			
21.0	0.35 (2)	12.0 (6)	13 (2) ^b	18 (2) ^b
23.3			13.6 (5)	16.4 (5)
25.0		16.4 (7)	13.5 (5)	16.4 (5)
25.8	0.49 (2)			

^a In 0.1 M (1-Bu)₄NBF₄/acetone solution with 2 mM electroactive species. ^b Averaged over four runs. ^c Averaged over three runs.

triflate⁹ in either the Ru(III) or Ru(II) complexes. Similar reactions involving the aqua ligand were also ruled out by examining the electrochemistry of $[\text{Ru}(\text{NH}_3)_5(\text{OH}_2)](\text{CF}_3\text{SO}_3)_3$ in acetone. The resulting redox couple (-410 mV vs Fc^+/Fc) is clearly distinguishable from those assigned to the two redox couples of the acetone complexes. In fact, under the experimental conditions used, the conversion of the aqua complex to the acetone complex can be monitored electrochemically and is complete within 10 min at 21 °C. The addition of $\text{Zn}(\text{CF}_3\text{SO}_3)_2$ also indicates that the Zn^{2+} produced during the in situ reduction of Ru(III) by $\text{Zn}(\text{Hg})$ does not interfere with the redox chemistry.

Using a nonisothermal cell, the rate and equilibrium constants were measured over a temperature range of $-25 \rightarrow +25$ °C for the Ru(II) $\eta^1 \rightarrow \eta^2$ isomerization and a range of $0 \rightarrow 25$ °C for the Ru(III) $\eta^2 \rightarrow \eta^1$ isomerization (Table IV). The smaller temperature range available to these techniques for the Ru(III) reactions was limited by the slowness of the reaction below 0 °C and by interference from the condensation reaction to form diacetone alcohol complexes at temperatures higher than 25 °C. From the temperature dependencies of k_1 and k_2 , the enthalpies and entropies of activation were calculated for the $\eta^1 \rightarrow \eta^2$ isomerization of $[\text{Ru}(\text{NH}_3)_5(\text{OC}(\text{CH}_3)_2)]^{2+}$ to be 63 ± 1 kJ mol^{-1} and -10 ± 2 $\text{J K}^{-1} \text{mol}^{-1}$, while for the $\eta^2 \rightarrow \eta^1$ isomerization of $[\text{Ru}(\text{NH}_3)_5(\text{OC}(\text{CH}_3)_2)]^{3+}$ they were found to be 48 ± 2 kJ mol^{-1} and -91 ± 7 $\text{J K}^{-1} \text{mol}^{-1}$, respectively. The enthalpies and entropies

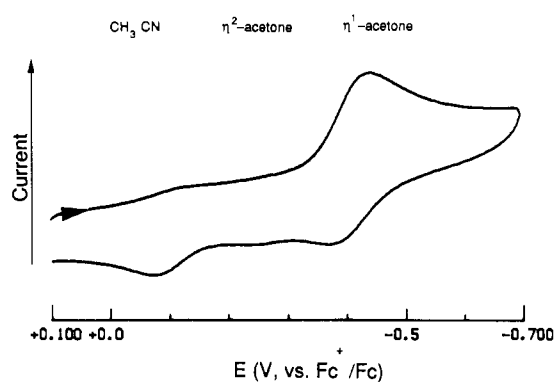


Figure 3. Cyclic voltammogram of $[\text{Ru}(\text{NH}_3)_5(\text{OC}(\text{CH}_3)_2)]^{3+/2+}$ in 50% v/v acetonitrile/acetone at 3 °C and 250 mV s^{-1} (2 mM electroactive species, 0.1 M (1-Bu)₄NBF₄). The small reduction wave for the $[\text{Ru}(\text{NH}_3)_5(\text{NCCH}_3)]^{3+}$ complex on the initial scan is due to the relatively slow ligand exchange of the Ru(III) complex at these temperatures. It is absent if the CV is run immediately upon dissolution.

for the two isomerizations (Table III) were calculated from the temperature dependencies of the equilibrium constants.

Using ¹H NMR spectroscopy, the rate constant of exchange of coordinated acetone with the deuterated solvent in the Ru(III) complex, at 0 °C, was found to be $(6.9 \pm 0.5) \times 10^{-6} \text{ s}^{-1}$, which is much smaller than the Ru(III) $\eta^1 \rightarrow \eta^2$ isomerization rate constant at that temperature, $(4.3 \pm 0.4) \times 10^{-3} \text{ s}^{-1}$. At 5 °C, the two rates were found to be $(1.3 \pm 0.3) \times 10^{-5} \text{ s}^{-1}$ and $(6.7 \pm 0.4) \times 10^{-3} \text{ s}^{-1}$, respectively.

From the cyclic voltammetry of $[\text{Ru}(\text{NH}_3)_5(\text{OC}(\text{CH}_3)_2)](\text{CF}_3\text{SO}_3)_3$ dissolved in 50% v/v acetone/acetonitrile at 3 °C (Figure 3), the rate constants for the substitution of η^1 -coordinated acetone by acetonitrile and the $\eta^1 \rightarrow \eta^2$ isomerization, both in the Ru(II) oxidation state, were found to be 0.4 s^{-1} and 0.3 s^{-1} , respectively. When the acetone complex was first dissolved in this solvent mixture at 3 °C, it exhibited a single reversible couple (at 10.2 V s^{-1}), indicating the $\geq 90\%$ purity of the Ru(III) acetone complex. At the slower scan rates, the oxidative scan resulted in peaks due to η^1 -acetone, η^2 -acetone, and η^1 -acetonitrile complexes (Figure 3). The peak current due to the oxidation of $[\text{Ru}(\text{NH}_3)_5(\text{NCCH}_3)]^{2+}$ was about 5 times larger than that due to $[\text{Ru}(\text{NH}_3)_5(\eta^2\text{-OC}(\text{CH}_3)_2)]^{2+}$.

Upon dissolution of $[\text{Ru}(\text{NH}_3)_5(\text{OSO}_2\text{CF}_3)](\text{CF}_3\text{SO}_3)_2$ in acetone at -23 °C, the cyclic voltammetry (at 1003 mV s^{-1}) revealed a reversible redox couple at -494 ± 6 mV (Fc^+/Fc), which was assigned to the $[\text{Ru}(\text{NH}_3)_5(\text{OSO}_2\text{CF}_3)]^{2+/+}$ couple. At slower scan rates, substitution of the triflate ligand by acetone was observed in the cyclic voltammetry (Figure 4) and the rate

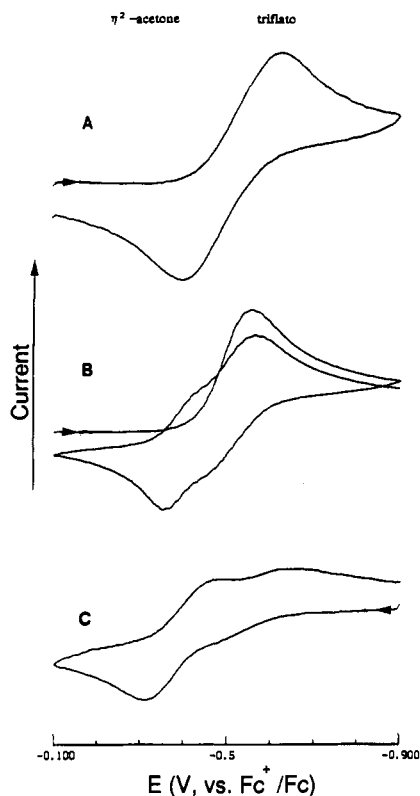


Figure 4. Cyclic voltammograms of $[\text{Ru}(\text{NH}_3)_5(\text{OSO}_2\text{CF}_3)]^{3+/2+}$, in acetone at -23°C , vs Fc^+/Fc (2 mM electroactive species in 0.1 M (1-Bu) $_4\text{NBF}_4$): A, $[\text{Ru}(\text{NH}_3)_5(\text{OSO}_2\text{CF}_3)]^{2+}$ at 10.2 V s^{-1} ; B, $[\text{Ru}(\text{NH}_3)_5(\text{OSO}_2\text{CF}_3)]^{2+}$ at 1003 mV s^{-1} ; C, $[\text{Ru}(\text{NH}_3)_5(\text{OSO}_2\text{CF}_3)]^+$ at 5.12 V s^{-1} . The larger peak-to-peak separations for curves A and C are due to heterogeneous electron transfer and/or residual uncompensated resistance at these low temperatures.

constant was calculated, using both methods, to be $1.2 \pm 0.2\text{ s}^{-1}$ at -23°C . This compares with an isomerization rate ($\text{Ru}(\text{II})\ \eta^1 \rightarrow \eta^2$) of $0.109 \pm 0.002\text{ s}^{-1}$, at the same temperature.

Using the nonisothermal cell results, the entropies of the reductions, $\Delta S^\circ_{\text{rc}}$, were calculated. For the $[\text{Ru}(\text{NH}_3)_5(\eta^1\text{-OC}(\text{CH}_3)_2)]^{3+/2+}$ couple, $\Delta S^\circ_{\text{rc}}$ is $112 \pm 6\text{ J K}^{-1}\text{ mol}^{-1}$, while, for the $[\text{Ru}(\text{NH}_3)_5(\eta^2\text{-OC}(\text{CH}_3)_2)]^{3+/2+}$ couple, it is $107 \pm 7\text{ J K}^{-1}\text{ mol}^{-1}$. Thermodynamic data for the cross-reaction (Scheme I) have been calculated from the dependence of $(E_1 - E_2)$ upon temperature; the free energy, ΔG° , the enthalpy, ΔH° , and the entropy, ΔS° , were found to be $-13.6 \pm 0.5\text{ kJ mol}^{-1}$, $-14 \pm 1\text{ kJ mol}^{-1}$, and $-5 \pm 7\text{ J K}^{-1}\text{ mol}^{-1}$, respectively.

Discussion

Satisfactory microanalyses were not obtained for the Ru(III) and Ru(II) acetone complexes because of their sensitivity to moisture, O_2 , and N_2 (for Ru(II)) and the thermal loss of acetone from the coordination sphere in the solid state. However, the spectroscopic and electrochemical results indicate purities of $\geq 90\%$ for the isolated solids. This was determined from the comparison of the peak integration of the released acetone with the NH_3 resonances in the $^1\text{H NMR}$ spectra. In the case of Ru(III), it was also confirmed by the presence of only a single reversible Ru(III)/Ru(II) couple when the complex was dissolved in acetone/acetonitrile at temperatures sufficiently low that substitution is slow within the time scale of the experiment. Since all other complexes which could be impurities exhibit distinctly different Ru(II)/Ru(III) couples, they would be observed in these experiments.

Spectroscopy. The η^1 -coordination of acetone in $[\text{Ru}(\text{NH}_3)_5(\text{OC}(\text{CH}_3)_2)](\text{CF}_3\text{SO}_3)_3$ results in a shift of the $\text{C}=\text{O}$ stretch to a lower wavenumber by 35 cm^{-1} . This small value is consistent with the relatively undistorted $\text{C}=\text{O}$ bond but shows

that the resonance is due to coordinated acetone and not acetone of crystallization. The weak intensity of the Ru(III) $\text{C}=\text{O}$ stretch is consistent with similar observations on $[\text{Os}(\text{NH}_3)_5(\text{acetone})]^{3+}$. For the osmium complex, the $\text{C}=\text{O}$ stretch is so weak that it is not observed in the infrared spectrum, while it is quite strong for $[\text{Co}(\text{NH}_3)_5(\text{acetone})]^{3+}$.³⁰ The intermediacy of the intensity of the $\text{C}=\text{O}$ stretch in the Ru(III) complex, as opposed to the Co(III) and Os(III) complexes, is also consistent with similar observations made for coordinated nitriles in complexes with dinitrile ligands.³⁰ The intensities are explained, to a large degree, by the opposing effects of π -back-bonding and σ -bonding on the intensities.³⁰ The much larger shift observed for η^2 -coordination in $[\text{Ru}(\text{NH}_3)_5(\text{OC}(\text{CH}_3)_2)](\text{PF}_6)_2$, 438 cm^{-1} , is reminiscent of that for a range of (alkene)- and (alkyne)pentaammineruthenium(II) complexes, where $\Delta(\nu_{\text{CC}}) \sim 200\text{ cm}^{-1}$.³¹ Additionally, the shift is similar to that observed for the peak assigned to the $\text{C}=\text{O}$ stretch in $[\text{Ru}(\text{NH}_3)_5(\text{OC}(\text{CF}_3)_2)](\text{PF}_6)_2$ (440 cm^{-1} from that of the free hexafluoroacetone ligand). This ligand is only known to coordinate in an η^2 fashion.³² The shift in the Ru(II) $\text{C}=\text{O}$ stretch is due to the weakening of the carbonyl bond by the transfer of electron density from the $\text{C}=\text{O}$ bond to the ruthenium ion (σ -donation) and by π -back-bonding from the metal ion to the π^* acetone orbitals and is consistent with the affinity of ruthenium(II) for back-bonding.⁵ The $\text{M}^{\text{II}}\text{-N}$ stretches are expected to appear between 300 and 400 cm^{-1} ;³³ however, in the case of $[\text{Ru}(\text{NH}_3)_6]\text{Cl}_2$ it has been observed at 411 cm^{-1} ,³⁴ and for $[\text{Ru}^{\text{II}}(\text{NH}_3)_5(\text{NO}^+)]\text{Cl}_3$ it has been observed at 474 cm^{-1} .³⁵ It is thus likely that the peaks observed between 505 and 472 cm^{-1} for the Ru(II) complexes of acetone and hexafluoroacetone are due to the Ru-N stretches. The asymmetric peak at 255 cm^{-1} is consistent with the NRuN deformation.³⁴ The peak observed at 396 cm^{-1} in the far-IR region of $[\text{Ru}(\text{NH}_3)_5(\text{OC}(\text{CH}_3)_2)](\text{PF}_6)_2$ is characteristic of the $\text{M}-\pi$ -bond stretch and is similar to the value observed for the analogous hexafluoroacetone complex, the $\eta^1\text{ M}-\text{O}$ stretch is expected to occur at a lower frequency.³³ If the equilibrium between the η^1 and η^2 isomers of the Ru(II)-acetone complex is similar to that in solution, the weak peak observed at 1677 cm^{-1} can be assigned to the η^1 isomer. Its shift, by 15 cm^{-1} , to a lower wavenumber compared to the peak of the Ru(III) complex, is consistent with the greater degree of π -back-bonding in the Ru(II) complex.³⁶ The assignments of ν_{CO} for the Ru(III) and Ru(II) complexes are confirmed by the isotopic labeling experiments, where the calculated shifts were within error of the observed values.

While only one ammine peak is observable in the $^1\text{H NMR}$ spectrum of $[\text{Ru}(\text{NH}_3)_5(\text{OC}(\text{CH}_3)_2)](\text{CF}_3\text{SO}_3)_3$, the area of that peak is consistent with 12–15 protons. Given the uncertainty of integrating peaks that are so widely separated, it is not possible to say whether the trans ammine signal is superimposed upon the cis ammine peak, is too weak and broad to observe, or does not lie in the frequency range of the experiments ($-50 \rightarrow +250\text{ ppm}$). Another possibility is that the protons have exchanged with traces of water in the solvent. It is expected that the rate of proton exchange of ammine ligands trans to a weak σ -donor will be 2 or more orders of magnitude faster than for the cis ammine ligands.³⁷ Unfortunately, the addition of acid, such as $\text{CF}_3\text{SO}_3\text{H}$, to prevent such a reaction is not suitable in this situation because

(30) Johnson, A.; Taube, H. *J. Indian Chem. Soc.* **1989**, *66*, 503–511.

(31) Sullivan, B. P.; Baumann, J. A.; Meyer, T. J.; Salmon, D. J.; Lehmann, H.; Ludi, A. *J. Am. Chem. Soc.* **1977**, *99*, 7368–7370.

(32) Witt, M. *Adv. Inorg. Chem. Radiochem.* **1986**, *30*, 223–312.

(33) Nakamoto, K. *Infrared and Raman Spectra of Inorganic and Coordination Compounds*, 3rd ed.; Wiley-Interscience: New York, 1978; Chapter 3.

(34) Clucas, W. A. Unpublished results, 1989.

(35) Mercer, E. E.; McAllister, W. A.; Durig, J. R. *Inorg. Chem.* **1966**, *5*, 1881–1886.

(36) Clarke, R. E.; Ford, P. C. *Inorg. Chem.* **1970**, *9*, 227–235.

(37) Buckingham, D. A.; Foxman, B. M.; Sargeson, A. M. *Inorg. Chem.* **1970**, *9*, 1709–1725. Bramley, R.; Creaser, I. I.; Mackey, D. J.; Sargeson, A. M. *Inorg. Chem.* **1978**, *17*, 244–248.

it catalyzes other reactions of acetone. The position of the resonance assigned to the coordinated acetone is shifted downfield by 1.4 ppm relative to that of free acetone, which is consistent with that expected for a ligand attached to a paramagnetic center. Presuming that the Ru—O=C bond is angular, with inequivalent methyl groups, the presence of only one signal for the coordinated acetone indicates that there is rapid rotation around the Ru—O bond, resulting in identical chemical environments for the two methyls down to at least 0 °C.⁶

The position of the coordinated acetone resonance in the ¹H NMR spectrum of [Ru(NH₃)₅(η²-OC(CH₃)₂)](CF₃SO₃)₂ is characteristic of η²-coordinated acetone.⁶ The upfield shift of the coordinated acetone in the Ru(II) complex is smaller than that for the Os(II) complex (δ = 1.63 ppm),⁶ suggesting a weaker interaction between the metal and the acetone ligand in the case of Ru(II). At low temperatures, the cis ammine resonance was split, indicating that there is some steric interaction between the ligand methyl groups and the cis amines; this is in contrast to the Os(II) case, where splitting was not observed.⁶ Since the chemical shifts of the cis NH₃ resonances are temperature dependent, we cannot distinguish between the possibilities of freezing out a rotation around the Ru—η²-acetone bond at lower temperatures and simply separating peaks that are superimposed at room temperature. The latter possibility, i.e. that there is slow rotation about this bond at room temperature, seems unlikely; however, coalescence would occur anyway at room temperature because the coordinated acetone and solvent acetone are exchanging rapidly on the NMR time scale. In order to sort out these dynamic processes, it would be necessary to perform selective saturation experiments at low temperatures. What is clear is that the rotation of the acetone bound to Ru(II) is much slower than that of the acetone bound to Os(II), since no splitting of the cis NH₃ resonances is observed for the latter complex, even at very low temperatures.⁶ This highlights some differences between Ru(II) and Os(II). It is likely that the rapid rotation about the Os—η²-acetone bond is facilitated by the cis ammine ligands' being bent back considerably (as shown from the crystal structure⁶). The different type of bonding envisaged for the Ru(II) complex (see latter discussion) and the weaker Ru—η²-acetone bond are expected to cause smaller distortions in the coordination geometry and less sp³ character in the (CH₃)₂CO carbonyl carbon. Both factors will increase the steric clashes between the cis ammine groups and the CH₃ groups, thus slowing down the rate of rotation of the ligand in the Ru complex as compared to the Os complex, consistent with the ¹H NMR results.

It has been previously observed that there exists a dependence of the ¹H chemical shifts of the amines on the reduction potential of the complex. Both δ(NH) and E_{1/2} are indicators of the degree of π-back-bonding to the sixth ligand.²⁵ The chemical shifts observed here are intermediate between those of non-π-back-bonding ligands such as NH₃ and strongly π-back-bonding ligands such as alkenes,²⁵ supporting the proposed η² structure.

Electrochemistry. The reduction potential observed for the [Ru(NH₃)₅(η¹-OC(CH₃)₂)]^{3+/2+} couple relative to [Ru(NH₃)₆]^{3+/2+} is close to that of pentaammineruthenium(III/II) complexes of poor π-acceptor or non-π-acceptor ligands such as imidazole,³⁸ NH₃, and H₂O,³⁹ relative to the same standard. In the case of the [Ru(NH₃)₅(η²-OC(CH₃)₂)]^{3+/2+} reduction couple, the observed reduction potential is similar to that of the pentaamine(pyridine)ruthenium(III/II) couple,⁴⁰ which is a moderate π back-acceptor. The positive shift in the reduction potential is in accord with the results of a number of electrochemical studies which have indicated a link between the reduction potential and the ability of the sixth ligand in pentaammineruthenium(III/II)

complexes to π-back-bond.^{25,41} The reduction potential observed for the η² isomer is also similar to that of the η²-hexafluoroacetone complex. The latter has a somewhat more positive redox potential, indicative of a slightly greater degree of π-back-bonding for this ligand, since the electron-withdrawing abilities of the CF₃ substituents will stabilize π-back-bonding. These electrochemical and spectroscopic results support the conclusion that π-back-bonding is involved in stabilizing the η²-acetone complex.

The formation of the diacetone alcohol complexes in Ru(III) solutions but not in Ru(II) solutions is due to the stronger Lewis acidity of Ru(III), which causes the methyl protons to become acidic enough to self-catalyze the condensation with a solvent molecule. Similar observations have been made in Co(III) and Os(III) chemistry.^{6,42}

Kinetics and Thermodynamics. For the Ru(III) η¹-acetone and Ru(II) η²-acetone complexes, the scan-rate dependence of the reversibility of the two redox couples in acetone is characteristic of an ECEC mechanism (Scheme I).²⁹ For the Ru(III) isomerization, the relative values of the rate constants k₁ and k₋₁ compared with the rate constants of acetone exchange at the same temperature (from ¹H NMR spectroscopy) indicate that this isomerization occurs by an intramolecular pathway. In the case of the Ru(II) isomerization, the similarity between the value of k₂ and the rate constant of solvent substitution rules out an exclusively intramolecular process and indicates an intermolecular pathway, or at least that an intermolecular pathway is the major route to the isomerization. It is clear from Figure 3 that acetonitrile substitution in [Ru(NH₃)₅(η¹-OC(CH₃)₂)]²⁺ occurs more rapidly than the isomerization to [Ru(NH₃)₅(η²-OC(CH₃)₂)]²⁺, as judged from the oxidation currents of these two complexes on the anodic scan in 50% v/v acetonitrile/acetone. The larger peak current for the acetonitrile complex is accentuated because it is further away from the reduction of the Ru(III)-η¹-acetone complex and hence there is a longer time for substitution to occur before it is oxidized.

The change in the ratios of the [Ru(NH₃)₅(η¹-OC(CH₃)₂)]^{3+/2+} and [Ru(NH₃)₅(η²-OC(CH₃)₂)]^{3+/2+} couples in the multiple scans (Figure 3A) results from the differing values for the isomerization rates in the two oxidation states.

The very different values of ΔS[‡] observed for the two forward isomerizations indicate that there is a different mechanism acting in each isomerization, supporting the conclusions of the substitution studies. The small and negative entropy of activation observed in the linkage isomerization reaction of the Ru(II) complex is consistent with those observed for the substitution reactions of [M(NH₃)₅L]³⁺ in water.^{43,44} Therefore, it is consistent with a solvent-exchange mechanism. By contrast, the large negative value of ΔS[‡] for the Ru(III) isomerization is reminiscent of those values found for the substitution reactions of [M^{III}(NH₃)₅X]²⁺ complexes where X⁻ is an anionic leaving group. These large negative values are a result of electrostriction of solvent molecules as the charges separate.⁴⁵ This suggests that the transition state for the intramolecular linkage isomerization for the Ru(III) complexes has a structure that contains an appreciable percentage of the resonance structure shown in II. Such a charge-separated transition state (or tight ion pair) will be considerably stabilized by solvation with respect

(38) Johnson, C. R.; Henderson, W. W.; Shepherd, R. E. *Inorg. Chem.* **1984**, *23*, 2754–2763.

(39) Matsubara, T.; Ford, P. C. *Inorg. Chem.* **1976**, *15*, 1107–1110.

(40) Lim, H. S.; Barclay, D. J.; Anson, F. C. *Inorg. Chem.* **1972**, *11*, 1460–1467.

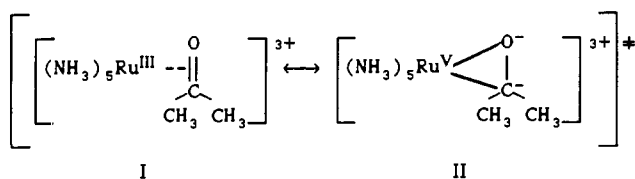
(41) Lancaster, J. C.; McWhinnie, W. R. *Inorg. Chim. Acta* **1971**, *5*, 515–519.

(42) Cordone, R.; Taube, H. Unpublished results, Stanford University. Lay, P. A. Unpublished results. Lay, P. A.; Magnuson, R. H.; Taube, H. *Inorg. Chem.* **1989**, *28*, 3001–3007.

(43) Lawrance, G. A.; van Eldik, R. *J. Chem. Soc., Chem. Commun.* **1987**, 1105–1106.

(44) Lawrance, G. A. *Inorg. Chem.* **1982**, *21*, 3687–3691.

(45) Tobe, M. I. In *Comprehensive Coordination Chemistry—The Synthesis, Reactions, Properties and Applications of Coordination Compounds*; Wilkinson, G., Gillard, R. D., McCleverty, J. A., Eds.; Pergamon: Oxford, U.K., 1987; Vol. 1, Chapter 7.1.



to I,⁴⁶ which could explain the large negative value of ΔS^\ddagger and the relatively small value of ΔH^\ddagger . It is unfortunate that the values from which ΔH^\ddagger and ΔS^\ddagger were derived are limited to a 25 °C temperature range by the experimental difficulties alluded to before. Therefore, ΔS^\ddagger for the Ru(III) reaction is known with much less accuracy than the Ru(II) value. Nonetheless, the quality of the data obtained from multiple runs suggests that a similar value of ΔS^\ddagger will be found if the rate constants are measured over a larger temperature range by other techniques.

The Electron-Transfer Cross-Reaction. For any square reaction scheme, there exists the added complication of the electron-transfer cross-reaction, where the minor isomer in the oxidized equilibrium oxidizes the minor isomer in the reduced equilibrium. For the system under study, the electron-transfer cross-reaction is shown in Scheme I. If this electron-transfer cross-reaction occurs, it can interfere with the calculations of the kinetic and thermodynamic results obtained from CV data for the square reaction scheme. However, the fact that the rate constants were observed to be independent of the concentration of the electroactive species indicates that the cross-reaction, which is a second-order reaction, cannot be interfering with the analysis to any significant extent.

The Triflate \rightarrow Acetone Substitution ECE Scheme. Upon dissolution of $[\text{Ru}(\text{NH}_3)_5(\text{OSO}_2\text{CF}_3)](\text{CF}_3\text{SO}_3)_2$ in acetone, at low temperatures, it is possible to observe the substitution of the triflate ligand by acetone. The substitution is observable due to the relatively inert nature of Ru(III) at these temperatures. Due to the limited amount of triflate present compared to acetone, the square scheme is not applicable, and an ECE mechanism fits the observed electrochemistry. The value obtained for the rate constant of substitution of triflate by acetone ($1.2 \pm 0.2 \text{ s}^{-1}$, at $-23 \text{ }^\circ\text{C}$) is an order of magnitude larger than that of the Ru(II) $\eta^1 \rightarrow \eta^2$ isomerization, at the same temperature (0.109 s^{-1}) and, by implication, that of the substitution by acetone. These results are also important in understanding the mechanism of isomerization for Ru(II). Since the η^1 -acetone complex is not observed upon reduction, this implies that direct coordination of acetone in an η^2 fashion is possible on a time scale that is faster than the $\eta^1 \rightarrow \eta^2$ isomerization. This supports the previous results that suggest that this isomerization is intermolecular, whereas the Os(II) isomerization is likely to be intramolecular. From crystal field considerations, an intermolecular process at Os(II) would be slower than one at Ru(II), which supports the above arguments. The observed substitution of the triflate ligand is an indication of the greater lability of the triflate ligand as compared to the η^1 -acetone ligand as a leaving group on Ru(II). It appears to be the first direct comparison of the relative leaving group ability of these ligands under identical conditions.⁴⁷

Alternative Explanations for an ECEC Mechanism. While the spectroscopy and electrochemistry strongly indicate the existence of $\eta^1 \leftrightarrow \eta^2$ linkage isomerizations, a number of other possibilities must be examined. It is possible that the square reaction scheme involves the reversible exchange of η^1 -acetone and some anion (CF_3SO_3^- or an anion from the electrolyte). Such a scheme would involve second-order kinetics, which is precluded by the fact that the observed rates were independent of the concentrations of the ruthenium complex (and hence $[\text{CF}_3\text{SO}_3^-]$), the electrolyte, and

added triflate. Additional evidence comes from the molar conductivity data, which indicate the presence of a sixth, neutral, ligand. Finally, the electrochemistry at low temperature shows that the $[\text{Ru}(\text{NH}_3)_5(\text{OSO}_2\text{CF}_3)]^{2+/+}$ couple occurs at potentials significantly different from those of the η^1 - and η^2 -acetone complexes.

The possibility of disproportionation of $[\text{Ru}(\text{NH}_3)_5(\eta^1\text{-acetone})]^{3+}$ following reduction to form $[\text{Ru}(\text{NH}_3)_5]^{2+}$ and other species, possibly a tetraammine, has been considered. This is precluded by the absence of a redox couple assignable to $[\text{Ru}(\text{NH}_3)_5]^{3+/2+}$, the presence of cis and trans ammine peaks in the ^1H NMR spectrum, and the stability of the electrochemistry over several cyclic voltammetric cycles.

With the recent characterization of the $[\text{Os}(\text{NH}_3)_5(\text{NH}=\text{C}(\text{CH}_3)_2)]^{2+}$ complex,⁴⁸ the possibility of a similar, but reversible, imine formation following the reduction of $[\text{Ru}(\text{NH}_3)_5(\text{OC}(\text{CH}_3)_2)]^{3+}$ must be considered. The absence of peaks assignable to the imine in both the infrared and the ^1H NMR spectra, together with the reversibility of the reaction over many cycles, indicates that this is not the case.

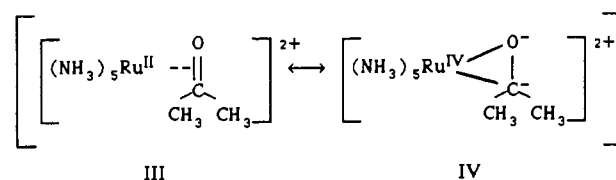
The possibility of oxidation-state-dependent reversible hydration of the acetone ligand by water impurities was also considered. However this possibility can also be discounted for the following reasons:

(i) Essentially the same rate constants were obtained when HPLC grade acetone was used and when AR grade acetone that had been distilled over $\text{KMnO}_4/\text{CaSO}_4$ or dried with activated alumina or silica gel powder was used. Since the amount of water in the acetone obtained from these sources would be variable, the reproducibility of the results is not consistent with a hydration mechanism.

(ii) Reversible hydration of the acetone ligand would be more activated for the Ru(III) than for the Ru(II) complex. However, the IR spectroscopic properties of the Ru(III) complex show clearly the presence of the acetone ligand, from the $\nu_{\text{C}=\text{O}}$ stretch at 1692 cm^{-1} , while the IR spectrum of the Ru(II) complex is inconsistent with an η^1 -acetone complex.

(iii) Acetone is rapidly and quantitatively released from the Ru(III) complex, which is inconsistent with the coordination of a *gem*-diol ligand, since alcohol ligands bound to Ru(III) are substitutionally inert.

Nature of the Bonding in the η^2 Complex. An η^2 bond can be described as a combination of two resonance forms, as illustrated in II and IV for the title complex. Resonance form III involves



the donation of the ketone π -bonding electron pair to the ruthenium, while IV involves the oxidative addition of the metal to the π bond of the ketone, yielding an oxametallacycle. The nature of the η^2 bond in a given complex depends on the relative importance of the ketone \rightarrow metal σ -donation and the metal \rightarrow ketone $d\pi\text{-}p\pi^*$ back-bonding. If the former predominates, then the η^2 bond approaches that of resonance form III, while if back-bonding predominates, then IV is the appropriate representation.

The η^2 -acetone complexes of Ru(II) and Os(II) show some marked differences in their spectroscopy and electrochemistry. These differences can perhaps be best explained in terms of the bonding scheme discussed above. The decrease in ν_{CO} of the acetone ligand in the Ru(II) complex is greater than that for the Os(II) analogue, indicating that the natures of the η^2 bonds are different in these two complexes, since Os(II) has a greater π -

(46) Lay, P. A. *Comments Inorg. Chem.* **1991**, *11*, 235–284. Lay, P. A.; Harman, W. D. *Adv. Inorg. Chem.* **1991**, *37*, 219–379.

(47) An indirect comparison has been made in the case of pentaamminecobalt(III).⁴

(48) Harman, W. D.; Taube, H. *Inorg. Chem.* **1988**, *27*, 3261–3262.

back-bonding ability.⁴⁶ The X-ray structure of the Os(II) complex indicates that it has a considerable contribution from the oxametallacycle resonance hybrid (resonance form IV),⁷ suggesting that the η^2 bond in the Ru(II) complex may involve a predominant contribution from resonance form III. An η^2 bond as in IV is expected to exhibit a M–O and a M–C stretch in the far-infrared region (separated by ~ 100 – 200 cm^{-1}), while one of type shown in structure III would exhibit a single M–(η^2 -C=O) stretch.³³ In the case of the Os(II) complex, the Os–O stretch has been reported,⁶ while, for the Ru(II) complex, only a single peak is observed, indicating the predominance of the type IV and III resonance forms, respectively, in the structures of the Os(II) and Ru(II) complexes.

The similarity of the reaction entropies for the two isomers of $[\text{Ru}(\text{NH}_3)_5(\text{OC}(\text{CH}_3)_2)]^{3+/2+}$ also supports the notion that the η^2 Ru(II) complex is predominantly of resonance form III, since the greater acidity of resonance hybrid IV would change the degree of solvent order and hence result in a very different value of $\Delta S^\circ_{\text{rc}}$ for an essentially Ru(V)/Ru(IV) couple compared to the Ru(III)/Ru(II) couple of the η^1 isomer. This preference of the Ru(II) complex for resonance form III and the Os(II) complex for IV also explains the quite different redox potentials observed for the two η^2 couples. In the osmium complex, which is closer to resonance form IV, the metal center approaches an Os(V)/Os(IV) couple and so would have a much more positive reduction potential than a structure in which resonance form III predominates. This would also explain the comparatively high reduction potentials of the ruthenium η^2 -alkene complexes compared to the acetone complex, because π -back-bonding is more important in the former.²⁵ Finally, the ^1H NMR experiments discussed earlier, which indicate much faster rotation about the M– η^2 -acetone bond for Os(II) in comparison to Ru(II), are also consistent with this analysis. The steric clashes between the planar acetone in resonance hybrid III are much larger than in structure IV, where the CH_3 groups are bent away from the NH_3 groups. Therefore, rotation about this bond is expected to be much slower in cases where resonance hybrid III predominates (i.e. Ru(II)) compared to cases where resonance hybrid IV is closer to the actual structure

(i.e. Os(II)). The observed difference in chemical reactivity between the Ru(II) and Os(II) acetone complexes is similar to that of the η^2 -benzene complexes $[\text{Os}(\text{NH}_3)_5(\eta^2\text{-C}_6\text{H}_6)]^{2+}$ and $[\text{Ru}(\text{NH}_3)_5(\eta^2\text{-C}_6\text{H}_6)]^{2+}$, where the former is moderately stable, while the latter is too unstable to detect.⁴⁹

From the infrared and electrochemical results, it is evident that while the Os(II) η^2 -acetone complex is stabilized to a large extent by π -back-bonding (IV), the corresponding Ru(II) complex is stabilized mainly by σ -donation (III). These results contrast with the S \leftrightarrow O linkage isomerization reactions of the $[\text{M}(\text{NH}_3)_5(\text{dmsO})]^{3+/2+}$ complexes, where the mechanisms for stabilization of the complexes by Ru and Os are expected to be similar and the observed kinetic and thermodynamic data do not differ greatly between the metal ions.^{50–52}

Implications for the Use of $[\text{Ru}(\text{NH}_3)_5(\text{OC}(\text{CH}_3)_2)]^{2+}$ as a Synthetic Intermediate. The rate constant of intermolecular isomerization of $[\text{Ru}(\text{NH}_3)_5(\text{OC}(\text{CH}_3)_2)]^{2+}$ found in this work is of the same order of magnitude as the estimated³ rate constant of aqua exchange in $[\text{Ru}(\text{NH}_3)_5(\text{OH}_2)]^{2+}$. These results indicate that the similarity in rate of substitution of the acetone ligand in acetone compared to the aqua ligand of $[\text{Ru}(\text{NH}_3)_5(\text{H}_2\text{O})]^{2+}$ in water is due to the predominance of the η^2 -bound acetone isomer, which is more inert than the η^1 isomer.

Acknowledgment. This work was supported by a grant from the Australian Research Council. We are also grateful for the assistance provided by Jacque Nemorin, Les Field, and Bruce Rowe in obtaining and interpreting the NMR experiments, to Henry Taube for providing information on the Os(II) η^2 -acetone complex and ref 30, prior to publication, and to James Mayer for information on $[\text{W}(\eta^2\text{-OC}(\text{CH}_3)_2)_2\text{Cl}_2(\text{PMePh}_2)_2]$.

Supplementary Material Available: A table illustrating the temperature dependence of the redox potentials of $[\text{Ru}(\text{NH}_3)_5(\eta^1\text{-OC}(\text{CH}_3)_2)]^{3+/2+}$ and $[\text{Ru}(\text{NH}_3)_5(\eta^2\text{-OC}(\text{CH}_3)_2)]^{3+/2+}$ (2 pages). Ordering information is given on any current masthead page.

(49) Harman, W. D.; Taube, H. *J. Am. Chem. Soc.* **1988**, *110*, 7555–7557.

(50) Yeh, A.; Scott, N.; Taube, H. *Inorg. Chem.* **1982**, *21*, 2542–2545.

(51) Harman, W. D. Ph.D. Thesis, Stanford University, 1987.

(52) Lay, P. A.; Taube, H. Unpublished results, 1982.